A mechanistic model of $H_2{}^{18}O$ and $C^{18}OO$ fluxes between ecosystems and the atmosphere: Model description and sensitivity analyses

W. J. Riley,[1] C. J. Still,[2,3] M. S. Torn,[1] and J. A. Berry[4]

Received 31 January 2002; revised 2 May 2002; accepted 9 May 2002; published 21 November 2002.

[1] The concentration of ^{18}O in atmospheric CO_2 and H_2O is a potentially powerful tracer of ecosystem carbon and water fluxes. In this paper we describe the development of an isotope model (ISOLSM) that simulates the ^{18}O content of canopy water vapor, leaf water, and vertically resolved soil water; leaf photosynthetic $^{18}OC^{16}O$ (hereinafter $C^{18}OO$) fluxes; CO_2 oxygen isotope exchanges with soil and leaf water; soil CO_2 and $C^{18}OO$ diffusive fluxes (including abiotic soil exchange); and ecosystem exchange of $H_2{}^{18}O$ and $C^{18}OO$ with the atmosphere. The isotope model is integrated into the land surface model LSM, but coupling with other models should be straightforward. We describe ISOLSM and apply it to evaluate (1) simplified methods of predicting the $C^{18}OO$ soil-surface flux; (2) the impacts on the $C^{18}OO$ soil-surface flux of the soil-gas diffusion coefficient formulation, soil CO_2 source distribution, and rooting distribution; (3) the impacts on the $C^{18}OO$ fluxes of carbonic anhydrase (CA) activity in soil and leaves; and (4) the sensitivity of model predictions to the $\delta^{18}O$ value of atmospheric water vapor and CO_2. Previously published simplified models are unable to capture the seasonal and diurnal variations in the $C^{18}OO$ soil-surface fluxes simulated by ISOLSM. Differences in the assumed soil CO_2 production and rooting depth profiles, carbonic anhydrase activity in soil and leaves, and the $\delta^{18}O$ value of atmospheric water vapor have substantial impacts on the ecosystem CO_2 flux isotopic composition. We conclude that accurate prediction of $C^{18}OO$ ecosystem fluxes requires careful representation of $H_2{}^{18}O$ and $C^{18}OO$ exchanges and transport in soils and plants. *INDEX TERMS:* 0315 Atmospheric Composition and Structure: Biosphere/atmosphere interactions; 1615 Global Change: Biogeochemical processes (4805); 1655 Global Change: Water cycles (1836); 1818 Hydrology: Evapotranspiration; *KEYWORDS:* 18O in CO2, model, 18O in H2O, isotope model, ecosystem model, land surface model

Citation: Riley, W. J., C. J. Still, M. S. Torn, and J. A. Berry, A mechanistic model of $H_2{}^{18}O$ and $C^{18}OO$ fluxes between ecosystems and the atmosphere: Model description and sensitivity analyses, *Global Biogeochem. Cycles*, *16*(4), 1095, doi:10.1029/2002GB001878, 2002.

1. Introduction

[2] Our ability to predict climatic impacts of anthropogenic activity depends on an understanding of the biological and biophysical processes that interact with atmospheric CO_2. Terrestrial gross carbon fluxes (i.e., photosynthesis and soil-microbial and plant respiration, which together comprise net ecosystem exchange) respond differently to environmental conditions such as air and soil temperature, moisture, and vegetation type. Unraveling the impacts of these forcing factors on the gross fluxes and net ecosystem carbon exchange requires mechanistic understanding of the processes involved and inclusion of these mechanisms in terrestrial biosphere models. In this context, the oxygen isotopic composition of atmospheric CO_2 may prove particularly helpful. Unlike the concentration and $\delta^{13}C$ value of atmospheric CO_2, which are tightly coupled and largely sensitive to net carbon exchanges, the $\delta^{18}O$ value of atmospheric CO_2 can aid in the distinction of gross fluxes because of the large differences between photosynthetic and soil respiratory isotopic signatures [*Keeling*, 1995; *Yakir and Wang*, 1996].

[3] *Francey and Tans* [1987] and *Friedli et al.* [1987] originally described the importance of terrestrial gross fluxes in determining variations in the $\delta^{18}O$ value of atmospheric CO_2. To better constrain the $\delta^{18}O$ value of soil-respired CO_2, *Hesterburg and Siegenthaler* [1991] developed a model of the hydration and isotopic equilibration with soil water of CO_2 as it diffuses through the soil column. They also demonstrated that competition between

[1]Earth Sciences Division, Lawrence Berkeley National Laboratory, Berkeley, California, USA.
[2]Berkeley Atmospheric Sciences Center, University of California, Berkeley, California, USA.
[3]Currently at Department of Geography, University of California, Santa Barbara, California, USA.
[4]Department of Plant Biology, Carnegie Institution of Washington, Stanford, California, USA.

0886-6236/02/2002GB001878$12.00

diffusion and equilibration with soil water determines the $\delta^{18}O$ value of soil-respired CO_2. *Tans* [1998] and *Miller et al.* [1999] extended this work by incorporating the influence of an abiotic "invasion" flux on the soil-surface $^{16}OC^{18}O$ (hereinafter $C^{18}OO$) flux.

[4] *Farquhar et al.* [1993] and *Farquhar and Lloyd* [1993] developed equations to describe photosynthetic exchanges of $C^{18}OO$. Analogous to soil respiration, CO_2 exchanges oxygen isotopes with water in the chloroplasts of leaves where photosynthetic carbon reduction occurs. *Farquhar et al.* [1993] demonstrated that these exchanges are a function of CO_2 fluxes into and out of stomata and catalysis of the hydration reaction by the chloroplastic enzyme carbonic anhydrase (CA). Other investigators have examined the details of these processes and their impacts on the $\delta^{18}O$ value of CO_2 fluxes during photosynthesis [*Flanagan et al.*, 1994; *Gillon and Yakir*, 2000a, 2000b; *Williams et al.*, 1996; *Yakir et al.*, 1994].

[5] The mechanistic understanding derived from these studies has been incorporated, to varying degrees, in global simulations of the $\delta^{18}O$ value of atmospheric CO_2. For example, *Ciais et al.* [1997a, 1997b] used a land surface model (SiB2) and an offline tracer-transport model (TM2) to examine the impacts of isotopic fluxes from vegetation and soils, ocean gas exchange, fossil fuel emissions, and biomass burning. They concluded that the seasonal cycle in the $\delta^{18}O$ value of atmospheric CO_2 is driven largely by terrestrial photosynthesis and respiration, while oceanic and anthropogenic sources have little effect. They also showed that the terrestrial biosphere drives the latitudinal gradient in the atmospheric $\delta^{18}O$ value, confirming the work of *Francey and Tans* [1987] and *Farquhar et al.* [1993]. Using the same combination of models as *Ciais et al.* [1997a], *Peylin et al.* [1999] showed that the high-latitude atmospheric CO_2 $\delta^{18}O$ seasonal cycle is largely a function of respiration from extratropical biomes, and that one region (the Siberian taiga) dominates most of the seasonality observed at remote, Northern Hemisphere monitoring stations.

[6] At the site level, *Yakir and Wang* [1996] took advantage of the isotopic difference between photosynthesis and soil respiration by using above-canopy measurements of ^{13}C and ^{18}O in CO_2 to partition net ecosystem exchange into its component fluxes. *Flanagan et al.* [1997] analyzed the influence of photosynthetic and respiratory carbon exchanges on the measured $\delta^{18}O$ value of CO_2 sampled in a forest canopy. In this study, diurnal variations in the $\delta^{18}O$ value of CO_2 were largely explained by variations in the photosynthetic $C^{18}OO$ fluxes. Another canopy-scale study [*Harwood et al.*, 1999] examined linkages between the plant and soil water pools with which CO_2 exchanges and the $\delta^{18}O$ value of canopy CO_2. They found that heterogeneity in the water pools likely accounted for variations in the $\delta^{18}O$ value of CO_2, and that these variations were not linked to the canopy CO_2 concentration.

[7] These global and canopy-scale studies demonstrate that the $\delta^{18}O$ value of CO_2 is a sensitive indicator of gross terrestrial carbon fluxes. However, the oxygen isotope exchanges of CO_2 with soil and plant water are mechanistically complex, temporally and spatially variable, and dependent on meteorological forcing and vegetation type and status (e.g., C_3 versus C_4 photosynthesis, leaf area index (LAI)). For example, C_3 grass leaves typically have higher internal CO_2 concentrations (c_i) than C_4 leaves. The effective fractionation across the leaf boundary layer and through the stoma depends on c_i, which in turn impacts the ecosystem CO_2 flux isotopic composition. Further, C_3 and C_4 plants differently affect the ecosystem energy and mass balances [*Baldocchi*, 1994].

[8] We contend that mechanistic representation in ecosystem models of the processes controlling $C^{18}OO$ and $H_2{}^{18}O$ fluxes will aid in our ability to use the $\delta^{18}O$ value of CO_2 as a tracer of ecosystem function. In particular, simulating integrated ecosystem water and carbon cycles is critical to predicting $C^{18}OO$ fluxes since these fluxes are strongly influenced by gross CO_2 fluxes and the isotopic composition of ecosystem H_2O pools. These integrated models will allow us to better constrain estimates of respiratory and photosynthetic CO_2 fluxes; improve our models of evaporation, transpiration, and energy balance partitioning; perform meaningful sensitivity studies; and test simplified models of isotopic exchange appropriate for large-scale simulations.

[9] In this paper we describe the development of a mechanistic model (called ISOLSM) to predict gross and net $C^{18}OO$ and $H_2{}^{18}O$ exchanges between ecosystems and the atmosphere. The isotope model has been integrated into the land surface model LSM (version 1.0) [*Bonan*, 1996] to allow fully coupled simulations of vegetation, soil, and atmospheric processes that are important in ecosystem fluxes. Modules are included to compute the $H_2{}^{18}O$ content of canopy water vapor, leaf water, and vertically resolved soil water; leaf photosynthetic and retrodiffusive $C^{18}OO$ fluxes; CO_2 equilibration with ^{18}O in soil water; and soil CO_2 and $C^{18}OO$ diffusive fluxes.

[10] The model has been tested using data collected at a C_4-dominated tallgrass prairie site (W. J. Riley et al, ^{18}O composition of CO_2 and H_2O ecosystem pools and fluxes in a tallgrass prairie: Simulations and comparisons to measurements, manuscript in preparation, 2002) (hereinafter referred to as Riley et al., manuscript in preparation, 2002). ISOLSM accurately predicted ecosystem CO_2 and latent and sensible heat fluxes; soil moisture and temperature; stem, leaf, and vertically resolved soil water isotopic composition; and the ecosystem CO_2 flux isotopic composition. We use forcing data from that study to drive the model for the tests and sensitivity analyses conducted here. However, the processes included in ISOLSM are applicable to other vegetation and soil types, and we intend to investigate the impacts of these factors on $C^{18}OO$ fluxes in future work. We are also integrating ISOLSM into an atmospheric GCM that captures diurnal variations in the ^{18}O composition of precipitation and boundary layer H_2O and CO_2 [*Noone et al.*, 2001].

[11] After describing the isotope modules and their integration we apply ISOLSM to evaluate (1) two previously published simplified methods of predicting $C^{18}OO$ soil-surface fluxes; (2) the impact of the soil-gas diffusion coefficient formulation and the assumed soil microbial CO_2 source and rooting distribution; (3) the impact of carbonic anhydrase (CA) activity in soil and leaves; and

(4) the sensitivity of model predictions to the $\delta^{18}O$ values of atmospheric water vapor and CO_2.

2. Model Description

[12] In this section we describe the pertinent relationships from LSM, modules integrated with LSM to simulate ecosystem $C^{18}OO$ and $H_2{}^{18}O$ exchanges, coupling of these modules within LSM, temporal and spatial discretization applied in the various submodels, and the solution methods applied. We express isotopic values in per mil (‰), with CO_2 flux and isotopic concentration ratios calculated relative to the standard Vienna Pee Dee belemnite (V-PDB), and H_2O isotopic values given relative to Vienna-Standard Mean Ocean Water (V-SMOW).

2.1. LSM

[13] LSM is a "big-leaf" [*Dickinson et al.*, 1986; *Sellers et al.*, 1996], single-canopy land surface model that simulates energy, CO_2, and H_2O fluxes between ecosystems and the atmosphere [*Bonan*, 1996, and references contained therein]. The model partitions the canopy into sunlit and shaded fractions. Separate modules are included to simulate aboveground fluxes of radiation, momentum, sensible heat, and latent heat; energy and water fluxes below ground; and coupled CO_2 and H_2O exchange between plants and the atmosphere. We applied the methods of *Reindl et al.* [1990] and *Alados and Alados-Arboledas* [1999] to partition the measured shortwave radiation into direct and diffuse components of visible and near-infrared radiation. As written, LSM runs on a subhourly time step for aboveground processes, while soil water transport is updated every 10 min. Twenty-eight surface types, comprising varying fractional land covers of 13 plant types, are simulated in the model. Soil hydraulic characteristics are determined from sand, silt, and clay content. For the examples presented here, we did not apply the LSM modules that predict ecosystem dynamics (e.g., LAI), but instead used measurements taken at the tallgrass site.

2.2. Soil Water and Heat Transport

[14] We made several changes to the hydrological routines in LSM to facilitate simulation of $H_2{}^{18}O$ fluxes between the ecosystem and atmosphere. The first change was to allow for varying soil hydrological properties with depth (i.e., hydraulic conductivity, water retention curve slope, and saturated water content). Although this change may be unnecessary for global simulations where information on vertically resolved soil hydrological properties is lacking, an ability to accommodate vertically resolved soil properties is valuable at the site scale.

[15] To simulate soil aqueous and gaseous transport, we required a finer spatial discretization than currently used in LSM. In ISOLSM, soil-water fluxes and $H_2{}^{18}O$ content are computed with a 300-s time step, half that currently used in LSM. We applied a 2.5-cm vertical discretization to 30 cm depth to resolve the near-surface soil water $H_2{}^{18}O$ gradient while maintaining a reasonable time step. The remainder of the soil column (down to 5 m) was discretized into nine progressively larger control volumes.

[16] LSM solves the Richards equation [*Warrick*, 2002] to determine the soil water content, θ (m^3 H_2O m^{-3} soil) and soil water flux, q (m^3 H_2O m^{-2} s^{-1}), as a function of depth, z (m), and time, t (s). The *Clapp and Hornberger* [1978] formulation is used to relate hydraulic conductivity and matric potential to the saturated hydraulic conductivity, saturated matric potential, and slope of the water retention curve. For the examples presented here we used measurements from the tallgrass prairie site for these parameters [*Colello et al.*, 1998].

[17] In LSM, if the predicted water content in a soil layer exceeds the saturated water content, θ_s (m^3 H_2O m^{-3} soil), the excess water is added to successive soil layers until each layer is brought to saturation. Also, if the predicted water content in a soil layer falls below a preset minimum, water is added to that layer from the layer below. While this strategy is appropriate for global simulations with stringent computational limits, discrepancies between the predicted soil moisture and water fluxes can occur during periods of high or low surface water inputs. Simulating $H_2{}^{18}O$ transport in soil water requires an internally consistent prediction of soil water content and fluxes between soil layers. To address this issue, ISOLSM recalculates the water flux based on the predicted water content at the end of each time step. LSM predicts the vertically resolved soil temperature, T_s (K), using a Fourier conduction model with moisture- and texture-dependent heat capacity and thermal conductivity.

2.3. Soil Water $H_2{}^{18}O$ Transport

[18] By mass balance, the depth-dependent ^{18}O soil water isotopic ratio, R_w, can be computed as

$$\frac{\partial(\mathrm{R}_w\theta)}{\partial t} = \frac{\partial(R_w q)}{\partial z} - R_w E_T, \tag{1}$$

where E_T (m^3 H_2O m^{-3} s^{-1}) is the transpiration flux partitioned into each soil layer based on the relative rooting density (ρ_r) and soil layer thickness. Note that equation (1) ignores diffusive transport (however, see *Mathieu and Bariac* [1996]) and that there is no isotopic fractionation for advective transport or root water withdrawal [*Bariac et al.*, 1994]. The vertical rooting density is assumed to be the same as a similar grassland site studied in the FIFE campaign [*Colello et al.*, 1998].

[19] Equation (1) is discretized on the same vertical grid as the soil moisture calculations and is solved explicitly at each time step. The surface flux boundary condition for equation (1) accounts for $H_2{}^{18}O$ inputs from rain and irrigation and the net $H_2{}^{18}O$ removed from the soil surface via evaporation. ISOLSM accounts for equilibrium fractionation during evaporation and fractionation through the laminar sublayer at the soil surface, as described below. For rain and irrigation inputs, the surface aqueous $H_2{}^{18}O$ flux is $q_i R_r$, where q_i (m^3 H_2O m^{-2} s^{-1}) is the infiltration rate and R_r is the incoming water isotopic concentration ratio. In the equations presented here, isotopic ratios (R) are defined as the ratio of the concentration of the rare species ($H_2{}^{18}O$ or $C^{18}OO$) to the sum of the rare and common species concentrations. In standard practice the measured concentration ratio of rare to common species is

typically substituted, and the difference is negligible [*Tans*, 1993]. To compare with measured values, we express computed values using this standard convention.

2.4. $H_2{}^{18}O$ Vapor Exchange

[20] In LSM, the canopy airspace is treated as a single compartment. The net ecosystem water vapor flux is computed from the water vapor gradient between canopy air and the atmosphere and a corresponding aerodynamic conductance. Analogously, we compute the $H_2{}^{18}O$ vapor flux, E^{18} (kg m^{-2} s^{-1}), between the ecosystem (plants and soil) and atmosphere as

$$E^{18} = E_g^{18} + E_v^{18,sun} + E_v^{18,sha} = \frac{\rho_a c_p}{\lambda\gamma}\left(R_a^v e_a - R_{atm}^v e_{atm}\right)c_a^{18}, \quad (2)$$

where ρ_a (kg m^{-3}) is air density; c_p (J kg^{-1} K^{-1}) is dry air heat capacity at constant pressure; λ (J kg^{-1}) is the latent heat of vaporization of water; γ (Pa K^{-1}) is the psychrometric constant, defined as $\lambda = \frac{c_p p_a}{0.622\lambda}$; p*a* is atmospheric pressure (Pa); R_{atm}^v and R_a^v are the atmospheric and canopy air water vapor ^{18}O isotopic ratios, respectively; e_{atm} and e_a (Pa) are the water vapor pressures in the atmosphere and canopy air, respectively; c_a^{18} (m s^{-1}) is the aerodynamic conductance for $H_2{}^{18}O$ (assumed to be the same as for H_2O); E_g^{18} (kg m^{-2} s^{-1}) is the soil-surface evaporative $H_2{}^{18}O$ flux; and the $H_2{}^{18}O$ fluxes from sunlit and shaded leaves, $E_v^{18,sun}$ and $E_v^{18,sha}$ (kg m^{-2} s^{-1}), are calculated as

$$E_v^{18,sun} = \frac{\rho_a c_p}{\lambda\gamma}\left(\alpha_e^w(T_v)R_l^{sun}e_i - R_a^v e_a\right)c_t^{18,sun} \quad (3)$$

$$E_v^{18,sha} = \frac{\rho_a c_p}{\lambda\gamma}\left(\alpha_e^w(T_v)R_l^{sha}e_i - R_a^v e_a\right)c_t^{18,sha}. \quad (4)$$

Here e_i (Pa) is the water vapor pressure within the leaf (i.e., saturated water vapor pressure, e_* (Pa), at the vegetation temperature, T_v (K)); R_l^{sun} and R_l^{sha} are the sunlit and shaded leaf water isotopic ratios, respectively; and $c_t^{18,sun}$ and $c_t^{18,sha}$ (m s^{-1}) are the $H_2{}^{18}O$ conductances between the leaf interior and canopy air for sunlit and shaded leaves, respectively. The equilibrium vapor pressure offset above a liquid surface, α_e^w, is a function of temperature, T (K) [*Majoube*, 1971],

$$\alpha_e^w(T) = \frac{1}{\exp\left(\frac{1137}{T^2} - \frac{0.4156}{T} - 0.0020667\right)}. \quad (5)$$

[21] Following *Mathieu and Bariac* [1996], the soil-surface evaporative $H_2{}^{18}O$ flux is calculated as

$$E_g^{18} = \frac{\rho_a c_p}{\lambda\gamma}\left(\alpha_e^w\left(T_{s,0}\right)R_{w,0}e_*\left(T_{s,0}\right) - R_a^v e_a\right)c_g^{18}, \quad (6)$$

where $R_{w,0}$ and $T_{s,0}$ (K) are the soil water isotopic ratio and temperature in the top soil control volume, respectively, and c_g^{18} is the conductance between the soil surface and canopy air (m s^{-1}). Equation (6) defines the vapor flux boundary condition for equation (1). The $H_2{}^{18}O$ conductances applied in equations (2)–(6) are defined as

$$c_a^{18} = \frac{1}{r_{aw}}, \quad (7)$$

$$c_t^{18,sun} = (1 - f_w)\left\{\frac{L^{sun}}{\frac{r_b}{\alpha_{kb}} + \frac{r_s^{sun}}{\alpha_k}}\right\}, \quad (8)$$

$$c_t^{18,sha} = (1 - f_w)\left\{\frac{L^{sha}}{\frac{r_b}{\alpha_{kb}} + \frac{r_s^{sha}}{\alpha_k}}\right\}, \quad (9)$$

$$c_g^{18} = \frac{1}{r'_{aw} + \frac{r_{srf}}{\alpha_{kb}}}, \quad (10)$$

where α_k and α_{kb} are the water vapor isotopic kinetic fractionations for molecular diffusion and diffusion through a laminar boundary layer, respectively. These fractionations are calculated as the ratio of the $H_2{}^{18}O$ diffusivity, D_w^{18} (m^2 s^{-1}), to the H_2O diffusivity, D_w^{16} (m^2 s^{-1}), raised to an exponent n' : $\left(\frac{D_w^{18}}{D_w^{16}}\right)^{n'}$. *Merlivat* [1978] measured the ratio $\frac{D_w^{18}}{D_w^{16}}$ to be 0.97229. The exponent n' depends on turbulence intensity, ranging from 0.5 for fully turbulent conditions to 1.0 for pure molecular diffusion [*Mathieu and Bariac*, 1996]. In the simulations presented here we use $n' = 0.67$ for transport through the leaf and soil-surface boundary layers and $n' = 1.0$ for transport through the stoma. Resistances for H_2O and $H_2{}^{18}O$ in fully turbulent transport are taken to be identical. The remaining terms in equations (7)–(10) are as defined by *Bonan* [1996]; that is, f_w is the wetted fraction of the canopy; r_{aw} and r'_{aw} (s m^{-1}) are the aerodynamic resistances between the canopy air and atmosphere and between the ground surface and canopy air, respectively; r_s^{sun} and r_s^{sha} (s m^{-1}) are the sunlit and shaded stomatal resistances, respectively; $\overline{r}_b$ (s m^{-1}) is the leaf boundary layer resistance; L and S (m^2 m^{-2}) are the total leaf and stem area indices, respectively; and L^{sun} and L^{sha} (m^2 m^{-2}) are the sunlit and shaded leaf area indices, respectively.

[22] Combining equations (2), (3), (4), and (6) yields the following diagnostic equation for the canopy water vapor ^{18}O isotopic composition:

$$R_a^v = \frac{1}{e_a}\left[c_a^{18}R_{atm}^v e_{atm} + c_g^{18}\alpha_e^w\left(T_{s,0}\right)R_{w,0}e_*\left(T_{s,0}\right) + \alpha_e^w(T_v)e_i\left(R_l^{sun}c_t^{18,sun} + R_l^{sha}c_t^{18,sha}\right)\right] \cdot\left(c_a^{18} + c_g^{18} + c_t^{18,sun} + c_t^{18,sha}\right)^{-1}. \quad (11)$$

[23] In the examples described below we do not have continuous measurements of the atmospheric water vapor isotopic ratio, R_{atm}^v, which varies diurnally due to interactions with the canopy and overlying atmosphere. For this work, we assume atmospheric water vapor has a $\delta^{18}O$ value

of −10‰. This assumption recognizes the importance of the stemwater ^{18}O content and the dominant contribution of transpiration to the atmospheric boundary layer water vapor content. We examine the sensitivity of our predictions to this assumption below.

[24] An alternative (and simpler) method to equation (6) for computing the surface flux boundary condition is [*Ciais et al.*, 1997a]

$$E_g^{18} = \alpha_e^w(T_{s,0})R_{w,0}E_g. \tag{12}$$

In equation (12), the impact of evaporation on the near-surface soil water isotopic composition assumes that the $H_2{}^{18}O$ vapor flux can be calculated from the total soil evaporative flux and the equilibrium offset, without reference to the $H_2{}^{18}O$ vapor gradient between the surface and canopy air. We investigate below the impact of this assumption on the soil water isotopic composition and surface $H_2{}^{18}O$ and $C^{18}OO$ fluxes.

2.5. Soil Respiration

[25] To predict CO_2 and $C^{18}OO$ soil-surface fluxes, we require an estimate of the depth-dependent CO_2 source strength from microbial and root respiration, S_c (μmol m^{-3} s^{-1}). For the results presented here, we apply LSM's estimates of root respiration, r_r (μmol m^{-2} s^{-1}), and microbial respiration, r_m (μmol m^{-2} s^{-1}). Root respiration is computed as a function of root biomass and temperature, while microbial respiration depends on the average volumetric soil water content to 1 m depth, field capacity water content, saturation water content, soil carbon content, respiration rate at 10°C, and surface soil temperature. In future model updates we intend to include a more detailed representation of soil microbial processes to better quantify the soil-respired flux.

[26] The depth-dependent respiration source strength in the soil column is assumed to decay exponentially with depth such that the integrated source equals $r_m + r_r$:

$$S_c = \frac{r_m + r_r}{z_e} e^{-z/z_e}. \tag{13}$$

Here z_e (m) is the e-folding distance, taken to be 0.15 m for the baseline simulations. We investigate the sensitivity of the surface $C^{18}OO$ flux to z_e below.

2.6. CO_2 and $C^{18}OO$ Transport and Efflux

[27] Following *Tans* [1998], ISOLSM predicts the transient, depth-resolved soil gas-phase CO_2 concentration, C (μmol m^{-3}), as

$$\frac{\partial(\varepsilon_t C)}{\partial t} = \frac{\partial}{\partial z}\left(\varepsilon_a D_c \left(\frac{\partial C}{\partial z}\right)\right) + S_c. \tag{14}$$

Here $\varepsilon_t = \varepsilon_a + B\varepsilon_w$; ε_a and ε_w (m^3 m^{-3} soil) are the soil air- and water-filled pore space, respectively, and B (m^3 air m^{-3} water) is the temperature-dependent Bunson solubility coefficient. We calculate the depth-dependent CO_2 effective diffusivity, D_c (m^2 s^{-1}), as

$$D_c = D_0 \kappa \theta_s \left(\frac{\theta_s - \theta}{\theta_s}\right)^3 \left(\frac{T_s}{T_0}\right)^n, \tag{15}$$

where D_0 (m^2 s^{-1}) is the molecular diffusivity of CO_2 at T_0 = 298 K (1.4×10^{-5} m^2 s^{-1}) and κ is 0.66. *Moldrup et al.* [1999] developed the water content dependence in equation (15) using results from 29 undisturbed soils spanning a range of soil types. *Fuller et al.* [1966] found n to be about 1.75, while the Chapman-Enskog kinetic theory [*Bird et al.*, 2002], predicts a value of 1.5 for the temperature range expected in soils. Other investigators have applied different methods to estimate the effective soil gas diffusivity. We discuss the importance of the diffusivity formulation on the soil-surface CO_2 isotopic flux signature below.

[28] The soil-gas $C^{18}OO$ concentration can be calculated as [*Tans*, 1998]

$$\frac{\partial(\varepsilon_t R_g C)}{\partial t} = \frac{\partial}{\partial z}\left(\varepsilon_a D_c^{18}\left(\frac{\partial(R_g C)}{\partial z}\right)\right) + S_c R_s + k_H B \varepsilon_w C(R_{eq} - R_g), \tag{16}$$

where R_g is the gas phase CO_2 isotopic ratio; R_{eq} is the CO_2 isotopic ratio in equilibrium with local soil moisture (i.e., $R_{eq} = \alpha_e^c(T_s)R_w$); R_s is the isotopic ratio of the respired CO_2 (taken to be in equilibrium with the local soil moisture); k_H (s^{-1}) is the temperature-dependent hydration rate (equal to one-third the CO_2 hydration rate since there are three oxygen atoms present in the bicarbonate intermediate, i.e., $k_H = \frac{0.037}{3}\exp(0.118(T_s - 273.15 - 25))$ [*Skirrow*, 1975]); D_c^{18} (m^2 s^{-1}) is the effective $C^{18}OO$ diffusivity in the soil pore space, calculated as $\alpha_k^c D_c$; α_k^c is the isotopic kinetic fractionation for molecular diffusion of CO_2; and α_e^c is the temperature-dependent equilibration factor between gaseous CO_2 and water [*Brenninkmeier et al.*, 1983],

$$\alpha_e^c(T) = 1 + \frac{\left(\frac{17604}{T} - 17.93\right)}{1000}. \tag{17}$$

[29] The model ignores impacts of advective soil gas transport on the ^{18}O isotopic composition of soil-gas CO_2. *Stern et al.* [1999], in their numerical modeling study, showed that gas advection does not significantly impact the resulting soil-gas isotopic composition. We have assumed that CO_2 produced at depth in the soil is in equilibrium with local water. Respiration from roots in dry surface soil is a possible exception to this assumption, as the root tissue water may have an isotopic signature more similar to stem water. Macropore flow can be substantial in near-surface soils. The resulting increased effective diffusivity near the surface can reduce the effective kinetic fractionation of the CO_2 surface flux. Nevertheless, we did not explicitly consider near-surface macropore diffusive flow in this study, although the model structure allows the user to set the effective soil diffusivity as a function of depth, and thereby perform a sensitivity analysis of this process.

[30] The fluxes of $C^{18}OO$, F_s^{18} (μmol m^{-2} s^{-1}), and CO_2, F_s (μmol m^{-2} s^{-1}), from the soil surface are computed as

$$F_s^{18} = -\varepsilon_a D_c^{18} \left.\frac{\partial(R_g C)}{\partial z}\right|_{z=0} \tag{18}$$

$$F_s = -\varepsilon_a D_c \left.\frac{\partial C}{\partial z}\right|_{z=0}. \tag{19}$$

Note that equations (14) and (16) implicitly include the "invasion" (or "abiotic") flux. In the results presented here we impose the CO_2 concentration at the ground surface with measurements from the site and assume the surface CO_2 isotopic composition is 0.5‰. Equations (14) and (16) are solved using a Crank-Nicholson approach [*Press et al.*, 1989] for the diffusive term and an explicit approach for the source and reaction terms. The time step for these calculations is 60 s, and we used 20 unequal control volume sizes (more finely discretized near the surface) over the top 1 m of soil.

[31] Using the soil modules of ISOLSM in steady-state mode, we compared predicted soil CO_2 and $C^{18}OO$ concentrations and soil-surface fluxes with the analytical solutions presented by *Tans* [1998] for exponential and constant CO_2 source profiles. ISOLSM predictions of depth-resolved concentrations and fluxes were essentially identical to the steady-state analytical solutions (not shown).

2.7. Isotopic Composition of H_2O and CO_2 in Leaves and Stems

[32] We apply an equilibrium leaf water model [*Roden and Ehleringer*, 1999] to predict the leaf water isotopic ratio, R_l, for both sunlit and shaded leaves (i.e., R_l^{sun} and R_l^{sha}). The equilibrium model is based on the Craig-Gordon [*Craig and Gordon*, 1965] approach to predicting surface water isotopic composition, with modifications for leaves as described by *Flanagan et al.* [1991],

$$R_l = 1/\alpha_e^w(T_v)\left(\frac{1}{\alpha_k}R_{sw}\frac{(e_i-e_s)}{e_i}+\frac{1}{\alpha_{kb}}R_{sw}\frac{(e_s-e_a)}{e_i}+R_a^v\frac{e_a}{e_i}\right). \quad (20)$$

Here, e_s (Pa) is the water vapor pressure at the leaf surface and R_{sw} is the root-density-weighted soil water isotopic ratio, defined as

$$R_{sw} = \frac{\int R_w\rho_r dz}{\int \rho_r dz}, \quad (21)$$

where the integration covers the entire soil column. We assume that the plant stem water isotopic ratio equals R_{sw}.

[33] CA in plant leaves rapidly catalyzes CO_2 hydration and thereby accelerates ^{18}O exchange between CO_2 and plant water. Although previous models have assumed instantaneous CO_2 equilibration with plant water because of the presence of CA, recent work has shown that CA activity can vary among plant types, with the lowest activities in C_4 grasses [*Gillon and Yakir*, 2001; *Gillon and Yakir*, 2000a]. Further, *Helliker and Ehleringer* [2000] showed that bulk leaf water can be more enriched in ^{18}O in C_4 grass leaves than predicted by the Craig-Gordon model, and that the enrichment can vary along the length of the leaf. We assume here that gaseous CO_2 is in equilibrium with leaf and stem water at their respective temperatures, and therefore has isotopic ratios $R_{c,l} = \alpha_e^c(T_v)R_l$ and $R_{c,sw} = \alpha_e^c(T_{s,0})R_{sw}$, respectively. The impact of variable CA activity on $C^{18}OO$ exchange in leaves and soil will be examined below.

2.8. $C^{18}OO$ Exchanges in Leaves and Stems

[34] The $C^{18}OO$ fluxes into, F_{la}^{18} (μmol m^{-2} s^{-1}), and out of, F_{al}^{18} (μmol m^{-2} s^{-1}), sunlit and shaded leaves are calculated as

$$F_{la}^{18} = F_{la}R_{c,l}\alpha_k' \quad (22)$$

$$F_{al}^{18} = F_{al}R_{c,atm}\alpha_k', \quad (23)$$

where $R_{c,atm}$ is the atmospheric ^{18}O isotopic ratio of CO_2. Gross CO_2 fluxes into (F_{al} (μmol m^{-2} s^{-1})) and out of (F_{la} (μmol m^{-2} s^{-1})) the leaf are computed from the CO_2 concentrations in, and the resistance between, the atmosphere and leaf interior [*Ciais et al.*, 1997a]. The net $C^{18}OO$ leaf exchange (positive towards the atmosphere), F_{net}^{18} (μmol m^{-2} s^{-1}), is calculated as the difference between F_{la}^{18} and F_{al}^{18} on the sunlit and shaded fractions, weighted by the sunlit and shaded LAI fractions.

[35] The diffusive fractionation term, α_k', is the weighted fractionation across the laminar leaf boundary layer and through the stoma (ignoring the drawdown from the bottom of the stomatal pore to the chloroplast, which is about 0.8‰) [*Farquhar and Lloyd*, 1993],

$$\alpha_k' = \frac{(c_a-c_s)\alpha_{kb}^c+(c_s-c_i)\alpha_k^c}{c_a-c_i}. \quad (24)$$

Here α_{kb}^c is the isotopic kinetic fractionation for diffusion of CO_2 through the laminar leaf boundary layer (calculated analogously to H_2O), and c_a, c_i, and c_s are the CO_2 mole fractions in the canopy air, at the bottom of the stomatal pore, and at the leaf surface, respectively, as determined from the iterative photosynthesis and stomatal conductance calculation in LSM. Recent work by *Gillon and Yakir* [2000b] showed that the effective limit of CA activity is at the chloroplast surface adjacent to the mesophyll cell wall, rather than at the chloroplast interior. However, we do not calculate the concentration at the chloroplast surface, but instead apply the concentration at the bottom of the stomatal pore (c_i).

[36] $C^{18}OO$ fluxes from stem maintenance respiration, F_{sm}^{18} (μmol m^{-2} s^{-1}), and growth respiration, F_g^{18} (μmol m^{-2} s^{-1}), are calculated as

$$F_{sm}^{18} = F_{sm}R_{c,sw}\alpha_k^c \quad (25)$$

$$F_g^{18} = F_gR_{c,sw}\alpha_k^c, \quad (26)$$

where the stem maintenance respiration, F_{sm} (μmol m^{-2} s^{-1}), and growth respiration, F_g (μmol m^{-2} s^{-1}), are computed in LSM. We have applied molecular diffusive fractionation for stem maintenance and growth respiration, and assumed isotopic equilibrium with stemwater. The fraction of growth respiration occurring below ground is uncertain, although partitioning of growth respiration should track production of new tissue [*Amthor*, 1989]. Unfortunately, LSM does not simulate carbon allocation or other components of the soil carbon cycle. Integration of ISOLSM with the next generation of ecosystem models that include these processes will allow consistent partitioning of the growth respiration CO_2 flux. Note also that the

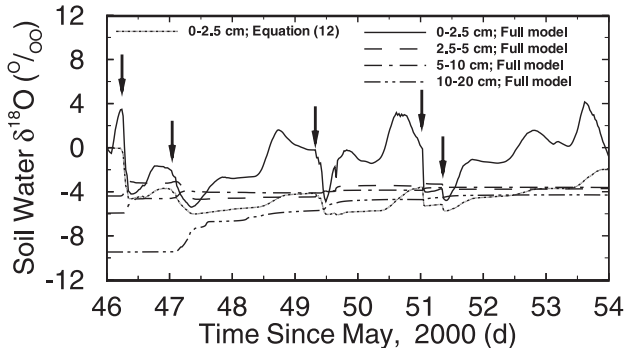

Figure 1. Soil water isotopic composition predicted by ISOLSM at four depth intervals and predicted by the method of equation (12) in the top 2.5 cm over a period with five precipitation events (indicated by the arrows). Differences between predictions from the full model and from equation (12) were small below the top soil layer. The $\delta^{18}O$ values are relative to the V-SMOW standard.

current version of ISOLSM does not account for isotopic exchange with canopy-intercepted or dew water.

[37] Finally, the net ecosystem $C^{18}OO$ flux, F^{18} (μmol m^{-2} s^{-1}), is computed as

$$F^{18} = F^{18}_{sm} + F^{18}_{g} + F^{18}_{net} + F^{18}_{s}. \quad (27)$$

3. Results and Discussion

[38] In this section we describe model performance for several model components, apply the model to evaluate two previously published methods of predicting the $C^{18}OO$ soil-surface flux, and examine the sensitivity of model predictions to several ecosystem parameters and functional representation of processes. We drive the model with the meteorological data set from the C_4-dominated tallgrass site between May and July 2000, as described by *Suyker and Verma* [2001].

3.1. Soil, Stem, and Leaf Water Isotopic Composition

[39] The soil-surface $H_2{}^{18}O$ evaporative flux depends on the top soil layer isotopic composition (equation (6)). In the absence of precipitation, the predicted soil water isotopic composition below the top layer remains relatively stable (Figure 1). Immediately following precipitation events (indicated by the arrows), the near-surface soil water isotopic composition approaches the isotopic composition of the precipitation. The extent to which a particular soil layer approaches the precipitation signal depends on the magnitude of the infiltration flux. Soil evaporation over the next few days causes the top soil layer's isotopic composition to become increasingly enriched in ^{18}O. Dynamics of the soil water isotopic composition will influence the soil-surface CO_2 flux isotopic composition (equation (16)).

[40] Applying the simplification described by equation (12) to compute the surface $H_2{}^{18}O$ vapor flux resulted in soil water isotopic compositions below the top soil layer (2.5 cm) within 1‰ of the full model predictions. However, in the top soil layer, the diurnal range and overall pattern of soil moisture isotopic composition differed between the two methods. During periods of moderate soil moisture the two methods predicted comparable mean diurnal isotopic compositions. During dry periods the method of equation (12) predicted top soil layer mean diurnal isotopic compositions up to 5‰ lighter than the full model. These differences between the two methods occur because of interactions between the soil surface and canopy airspace $H_2{}^{18}O$ vapor concentrations, which are accounted for in the full model but not in equation (12). The resulting soil-surface CO_2 flux isotopic composition differed by as much as 2‰ between the two methods.

[41] Predicted leaf water isotopic composition typically increases from early morning to midafternoon by between 10 and 20‰, and then relaxes back to a nighttime value by about midnight (Figure 2). During periods of high soil moisture and more frequent precipitation, the leaf water isotopic composition approaches the predicted stem water isotopic composition during the middle of the night. Note also that the predicted leaf water isotopic composition is more variable than the near-surface soil water over the afternoon.

[42] The depth distribution of root water uptake affects the predicted stem water isotopic composition, since deeper water tends to be isotopically lighter. We investigated the impact of this effect in two ways. First, we increased the rooting depth from 25 to 40 cm, while maintaining a comparable relative root density profile. The resulting stem water isotopic composition decreased by less than 1‰, while the leaf water isotopic composition and ecosystem $C^{18}OO$ flux were effectively unchanged. Second, we assumed that 40% of root water withdrawal was equally distributed over the top 15 cm and the remaining 60% was distributed over the next 15 cm. This distribution resulted in a daytime decrease of up to 2‰ in stem and leaf water isotopic compositions.

[43] We also examined the sensitivity of the net leaf $C^{18}OO$ exchange to leaf CA activity. In this test, we allowed the leaf CO_2 isotopic ratio, $R_{c,l}$, to change by a percentage (β) of the difference between the previous time step's value and the value computed assuming complete equilibrium (i.e., $\alpha^c_e(T_v)R_l$). Thus, over the simulation time step, β percent of the CO_2 molecules that could have equilibrated with leaf water were able to equilibrate. During the middle

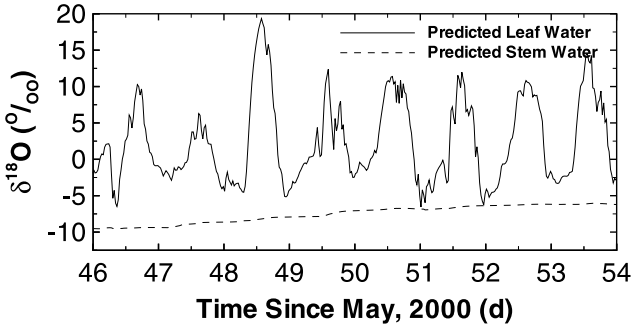

Figure 2. Predicted leaf and stem (source) water isotopic compositions. The $\delta^{18}O$ values are relative to the V-SMOW standard.

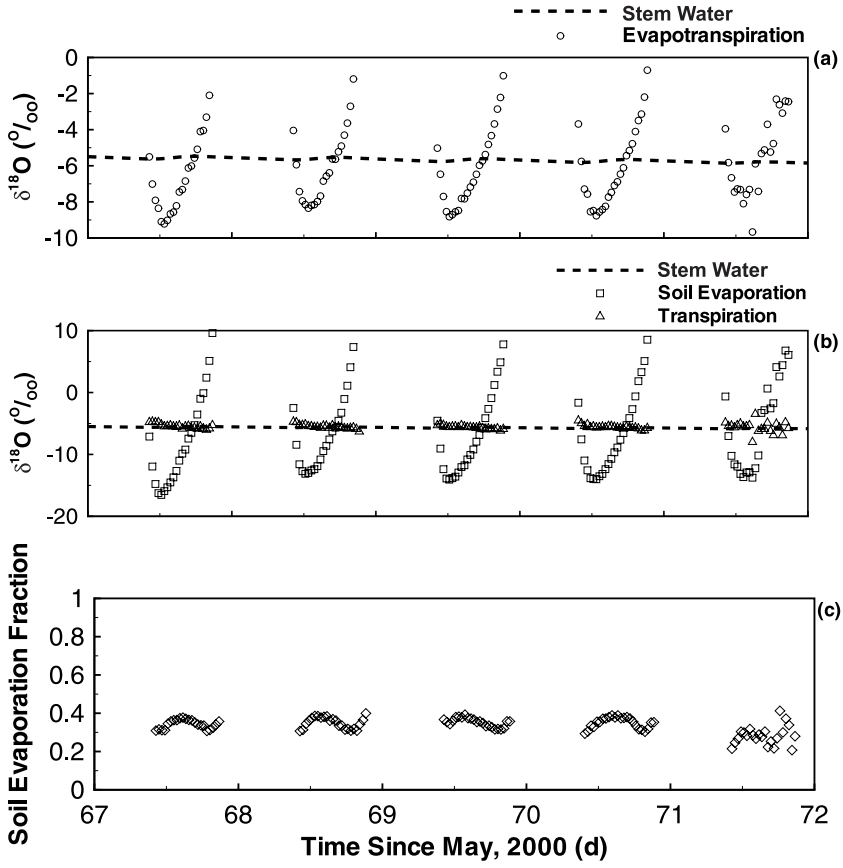

Figure 3. (a) Predicted ET flux and stem water isotopic composition. The simulation results are shown for periods when the ET flux is greater than 100 W m^{-2}. (b) Predicted isotopic compositions of the transpiration and soil evaporation fluxes. (c) Fraction of the ET flux accounted for by soil evaporation. The $\delta^{18}O$ values are relative to the V-SMOW standard.

of the day the net leaf flux isotopic composition was up to 5‰ different when CA activity was low (β = 20%) than when complete equilibrium was assumed (β = 100%). The simulations also show that the flux isotopic compositions are comparable when the leaf fluxes are small (early in the morning and at sundown).

[44] Prediction of the isotopic composition of ecosystem water pools depends on the assumed atmospheric H_2O isotopic composition. To examine model sensitivity to this parameter we varied the $\delta^{18}O$ value of atmospheric H_2O between -10 and -15‰. As expected, the lighter atmospheric water vapor content resulted in up to 5‰ lighter midday leaf and top soil layer water isotopic compositions. The impact diminished with soil depth, resulting in only about a 1‰ reduction in soil water isotopic composition between 10 and 20 cm. Predicted stem water isotopic composition was consistently 2‰ lighter throughout the simulation with the lighter atmospheric water vapor.

3.2. $H_2{}^{18}O$ Fluxes

[45] The predicted evapotranspiration (ET) flux isotopic composition is shown in Figure 3a for a 5-day period (predictions are shown when the ET flux is greater than 100 W m^{-2}). Also shown in Figure 3a is the predicted stem water isotopic composition. The predicted isotopic composition of the transpiration and soil evaporation fluxes are shown in Figure 3b. The transpiration flux matches the stem water isotopic composition, as required by the steady-state leaf water relationship (equation (20)), while the soil evaporative flux isotopic composition and fraction of the ET flux accounted for by soil evaporation (Figure 3c) vary diurnally and between days. Since the ET isotopic composition is a flux weighted average of soil evaporation and transpiration, the ET signature deviates from the stem water isotopic composition as a function of the soil evaporation fraction. This observation supports the idea that water vapor flux isotopic signatures can be used to partition ET between soil evaporation and transpiration [e.g., *Yakir and Wang*, 1996].

3.3. $C^{18}OO$ Soil-Surface Flux

[46] Studies by *Hesterburg and Siegenthaler* [1991], *Farquhar et al.* [1993], *Ciais et al.* [1997a], *Miller et al.* [1999], and *Stern et al.* [2001] suggested that the CO_2 surface flux isotopic composition can be estimated from an average near-surface soil water isotopic composition, a temperature-dependent equilibrium fractionation, and an effective kinetic fractionation. *Farquhar et al.* [1993] and *Ciais et al.* [1997a] solved global budgets of atmospheric $C^{18}OO$ to estimate the value of this effective fractionation.

Farquhar et al. [1993] suggested a value of 7.6‰, while *Ciais et al.* [1997a] inferred an effective kinetic fractionation of 5‰. In contrast, *Stern et al.* [2001] calculated, from the numerical model of *Tans* [1998], effective fractionation factors for a variety of biomes that range from about 0.7 to 9.6‰. *Miller et al.* [1999], from their detailed analysis of soil column measurements and model predictions, suggest using an effective kinetic fractionation of 7.2 ± 0.3‰ and the average soil water isotopic composition between 5 and 15 cm. To derive this value, they assumed an homogeneously distributed soil CO_2 production function. We examine the impact of the soil CO_2 production distribution below.

3.3.1. Comparison to Previous Approaches

[47] In Figure 4 we present a comparison between the surface CO_2 flux isotopic composition as predicted by ISOLSM and the two approximations described above. The simple model of *Ciais et al.* [1997a] (SM1) consistently overpredicts the full model results. The simple model of *Miller et al.* [1999] (SM2) and ISOLSM predict comparable mean diurnal CO_2 flux isotopic signatures during moderate soil moisture conditions. During periods immediately following a precipitation event, ISOLSM predicts a large change in near-surface soil water isotopic composition, which is reflected in a reduction in the soil-surface CO_2 flux isotopic composition. SM2 does not show these large reductions since the integrated soil water isotopic composition between 5 and 15 cm is relatively more stable. During sustained periods of dry soil, SM2 underestimates the flux isotopic signature by up to 5‰. Note that in contrast to SM1 and SM2, the soil-surface CO_2 flux isotopic composition as predicted by ISOLSM is dependent on the near-surface $C^{18}OO$ content. A sensitivity analysis indicates that the soil-surface CO_2 flux isotopic composition is relatively insensitive to this parameter.

3.3.2. Sensitivity Analyses

[48] We tested the impact of the CO_2 source profile on the soil-surface CO_2 flux isotopic composition by examining three scenarios: (1) CO_2 source distribution described by equation (13) and an e-folding depth of $z_e = 0.15$ m; (2) CO_2 source described by equation (13) and $z_e = 0.4$ m; and (3) a homogeneously distributed CO_2 source down to 0.4 m. The integrated CO_2 source through the soil column ($r_m + r_r$) was held constant for the three cases. For the cases with e-folding depths of 0.15 and 0.4 m, the soil-surface CO_2 flux isotopic composition was essentially unchanged during periods of high to moderate soil moisture. During dry soil conditions, the deeper CO_2 source profile resulted in up to a 2‰ lighter surface flux isotopic composition. This result reflects the larger fraction of the belowground CO_2 source in contact with lighter (deeper) soil water, and the competition between soil diffusion and isotopic exchange in the soil water. Analogously, imposing the homogeneously distributed source resulted in a surface flux isotopic composition up to 2 and 5‰ lighter than the first scenario during moderate to high and dry soil moisture conditions, respectively. Note that if the drier soils resulted in a more homogeneously distributed source, the SM2 model predictions would be in closer agreement with the full model during these periods. Because the soil CO_2 flux is small compared to gross photosynthesis in this system, the daytime ecosystem CO_2 flux isotopic composition was essentially unchanged by changing the CO_2 source profile.

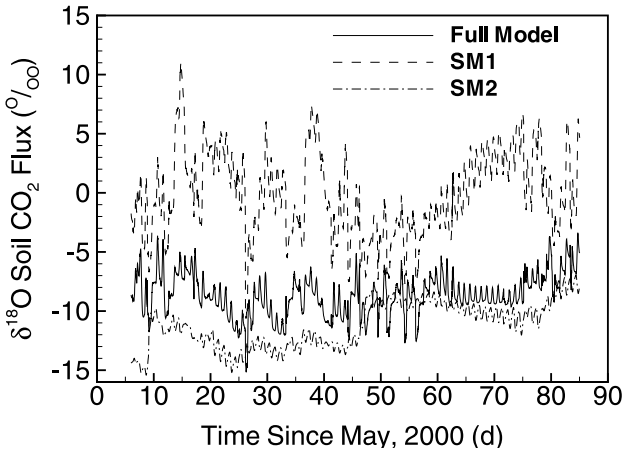

Figure 4. Predicted soil-surface CO_2 flux isotopic composition as predicted by ISOLSM and the methods of *Ciais et al.* [1997a] (SM1) and *Miller et al.* [1999] (SM2). The method of *Miller et al.* [1999] captures the flux isotopic composition during periods of moderate soil moisture but over predicts the isotopic composition during dry soil conditions. The $\delta^{18}O$ values are relative to the V-PDB standard.

[49] We investigated the sensitivity of the CO_2 flux isotopic composition to the method of calculating the diffusion coefficient by examining two scenarios: (1) the nominal case as described by the moisture dependence of equation (15); and (2) the commonly applied relationship [*Tans*, 1998]:

$$D_c^{16} = (\theta_s - \theta)\kappa D_0. \tag{28}$$

[50] The method of equation (28) predicted CO_2 surface-flux isotopic compositions about 1‰ lighter than the method of equation (15), although the diurnal patterns over the three-month period were unchanged. The diffusion coefficient predicted by equation (28) can be up to three times higher than that predicted by equation (15). Thus the flux associated with equation (28) is able to equilibrate with more of the deeper soil water than the flux associated with equation (15), resulting in the lighter flux isotopic composition. These observations are consistent with the steady state solutions presented by *Tans* [1998].

[51] The presence of CA or other soil catalytic processes could strongly affect the position in the soil column where CO_2 equilibrates with soil water. Recent work [*Atkins et al.*, 2001] indicates that the legume nodules associated with roots in nitrogen fixing trees have high CA concentrations. The impacts of these effects on the hydration rate, k_H, is uncertain and likely to vary with depth and location in the landscape. We investigated the sensitivity of the soil-surface CO_2 flux isotopic composition to this catalysis by increasing k_H by factors (α) of 20 and 1000 (Figure 5). Increasing k_H by a factor of 1000 did not substantially change the soil-surface flux isotopic composition above that of a factor of 100. The impact of the larger hydration rate increases as the

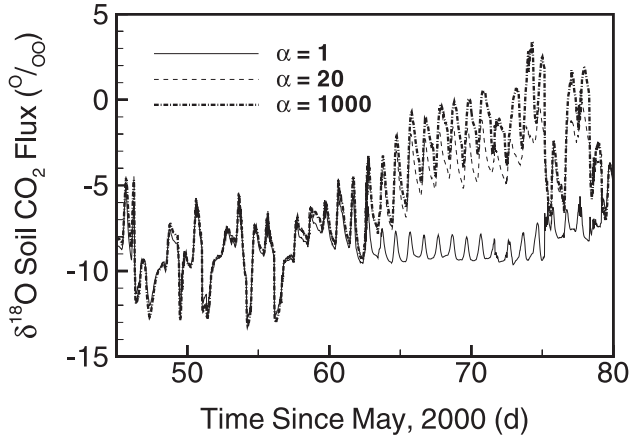

Figure 5. Impact of the CO_2 soil hydration rate, k_H, on the soil-surface CO_2 flux isotopic composition. Shown are predicted $\delta^{18}O$ values of the soil-surface CO_2 flux for nominal k_H, and for k_H increased by factors (α) of 20 and 1000. The impact of increasing the hydration rate is largest under dry soil moisture conditions (i.e., after day 62). The $\delta^{18}O$ values are relative to the V-PDB standard.

soil dries (e.g., days 65 through 80) and is small when the soil is wet (e.g., days 45 through 55). The higher soil moisture reduces the diffusion coefficient thereby allowing more time for equilibration with near-surface soil water and reducing the impact of variations in k_H.

3.4. $C^{18}OO$ Ecosystem Flux

[52] Figure 6a shows predicted leaf water and CO_2 flux isotopic compositions for a 5-day period in August 2000. Note that a negative $\delta^{18}O$ value for the ecosystem CO_2 flux implies that the ecosystem is enriching the atmosphere in ^{18}O (i.e., the lighter isotopomers are preferentially assimilated). At night, the ecosystem CO_2 flux signature remains relatively constant, since the soil water isotopic composition and the soil temperature are relatively constant. The sharp transitions in the morning and evening occur when the system switches between being dominated by respiration or photosynthesis. During the day, photosynthetic uptake and retrodiffusion dominate ecosystem carbon exchange. The predicted daytime CO_2 ecosystem flux isotopic signature typically begins light in the morning and increases by about 10‰ by late afternoon. This trend reflects the concurrent changes in leaf water isotopic composition and leaf discrimination [*Farquhar and Lloyd*, 1993] (Figure 6b).

[53] The net impact of the ecosystem fluxes on the atmospheric $C^{18}OO$ content is shown in Figure 6c. The isoflux, I (μmol m^{-2} s^{-1} ‰), is defined as

$$I = -(F_{AL} - F_{LA})\delta^c_{nl} + (F_g + F_{sm})\delta^c_{sw} + F_s\delta^c_s, \qquad (29)$$

where δ^c_{nl}, δ^c_{sw}, and δ^c_s correspond to the isotopic compositions of net leaf, stem respiration, and soil-surface CO_2 fluxes. Recall that during the night ISOLSM simulates, for the leaf, only a one-way maintenance respiration flux. Integrating the isoflux over each day results in daily fluxes of between 10 and 30 mol m^{-2} ‰. In this system the respiration isoflux is relatively small and consistent, while the photosynthetic isoflux varies strongly over the day and between days.

4. Summary and Conclusions

[54] We have developed a mechanistic model, called ISOLSM, to simulate $C^{18}OO$ and $H_2{}^{18}O$ fluxes between ecosystems and the atmosphere. ISOLSM includes modules that simulate transient canopy water vapor, leaf water, and vertically resolved soil water $H_2{}^{18}O$ content; leaf photosynthetic and retrodiffusive $C^{18}OO$ fluxes; and soil diffusive CO_2 and $C^{18}OO$ fluxes and equilibration with soil water. The isotope modules have been integrated into the land surface model LSM, although coupling with other land surface models should be straightforward. Model testing in a tallgrass prairie site is described in an upcoming paper (Riley et al., manuscript in preparation, 2002).

[55] Comparisons between ISOLSM and simplified models showed substantial differences between approaches, except under limited conditions. For example, the method of *Miller et al.* [1999] accurately captured the mean diurnal soil-surface CO_2 flux isotopic composition during periods of moderate soil moisture. However, during periods of dry soils the simple model predicted up to 5‰ lighter flux isotopic compositions.

[56] We evaluated model prediction sensitivity to several input parameters and mechanism formulations. Simulations indicate that CA activity in leaves and soil has large impacts on net leaf (up to 5‰) and soil-surface (up to 10‰) $C^{18}OO$ exchange. Varying the assumed rooting depth led to changes in the leaf and stem water isotopic compositions of up to 2‰. The soil CO_2 source profile most strongly affected the surface flux isotopic composition during periods of dry soil. The difference was largest when comparing an exponentially decaying source with an e-folding depth of 15 cm and a source that was constant to 40 cm depth. The deeper, constant source resulted in up to a 5‰ lighter CO_2 surface flux isotopic composition, reflecting equilibration with deeper, and therefore lighter, soil water. Note that in real systems, the respiration CO_2 production profile will depend on the depth-dependent soil moisture content and temperature. All else being equal, a drier soil will increase the effective production depth and result in soil water enriched in ^{18}O. The net effect of these mechanisms is difficult to discern without representing the coupled processes, as is done in ISOLSM. The soil-surface CO_2 flux isotopic composition was relatively insensitive to the formulations for the soil-gas diffusion coefficient. Finally, varying the $\delta^{18}O$ value of atmospheric H_2O had substantial impacts on the leaf, stem, and top soil layer water isotopic compositions, as well as on net ecosystem $C^{18}OO$ exchange.

[57] The work presented here highlights the impacts of various ecosystem processes on $C^{18}OO$ fluxes. The large variation in $C^{18}OO$ fluxes under changing environmental conditions implies that robust representation of processes important in soil and plant exchanges are necessary to accurately predict these fluxes. For example, leaf water isotopic composition strongly impacts $C^{18}OO$ net and

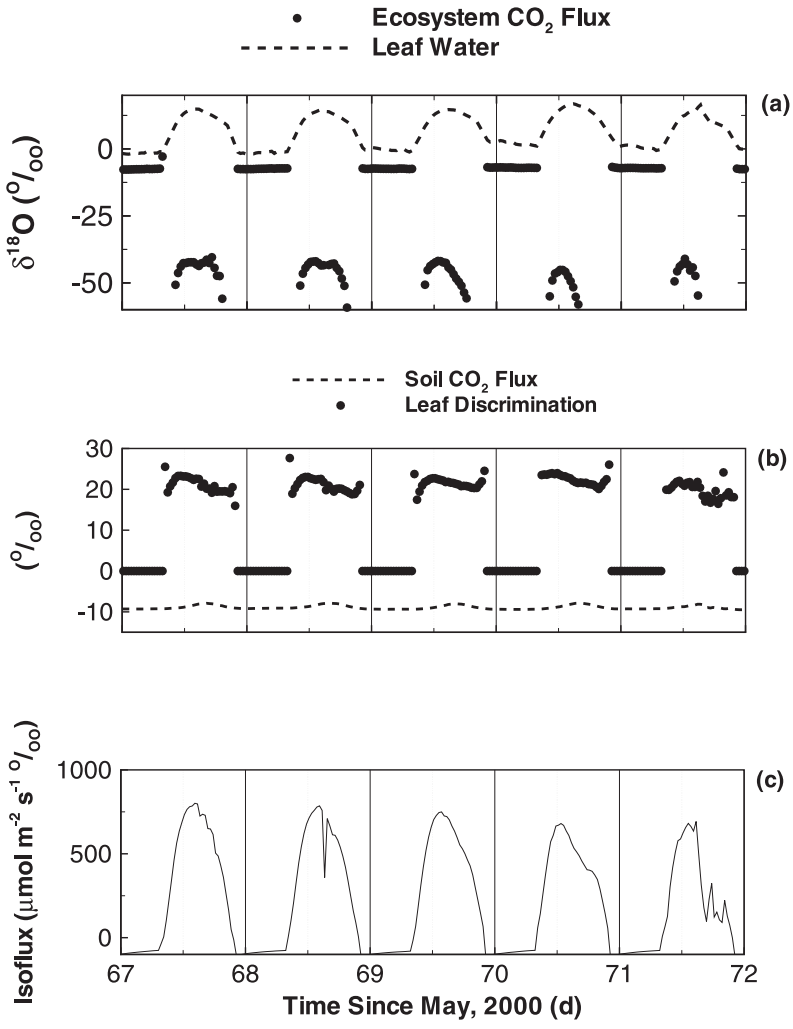

Figure 6. (a) Predicted ecosystem CO_2 flux and leaf water isotopic compositions. The CO_2 flux isotopic composition follows the leaf water signal, beginning light early in the morning, increasing until midafternoon and then declining until sundown. The CO_2 flux isotopic composition remains relatively constant at night. (b) Predicted soil-surface CO_2 flux isotopic composition and leaf discrimination. (c) Ecosystem flux. The $\delta^{18}O$ values for CO_2 fluxes and H_2O pools are relative to the V-PDB and V-SMOW standards, respectively.

retrodiffusive leaf fluxes. The leaf water isotopic composition depends on the root-activity weighted soil moisture isotopic composition, which depends on recent surface-water inputs and evaporative history. Failure to include these processes will likely result in inaccurate predictions of leaf water isotopic composition, and therefore inaccurate predictions of ecosystem $C^{18}OO$ fluxes. The simplified models of $C^{18}OO$ soil-surface fluxes that do not account for vertically resolved and transient soil moisture isotopic composition and respiration fluxes make substantially different predictions than models that include these effects. Thus, site-level and global forward and inverse models of respiratory and photosynthetic $C^{18}OO$ fluxes should benefit from ISOLSM's mechanistic representation of the land-surface isotopic flux balance. In future work we will apply ISOLSM to better understand the conditions under which separating respiratory and photosynthetic CO_2 fluxes using ^{18}O is possible, to better quantify the impact of environmental variability and parameter uncertainty on these flux estimates, and to develop simplified models of $C^{18}OO$ ecosystem exchanges appropriate for regional- and global-scale simulations.

Notation

B	Bunson solubility coefficient, m^3 air m^{-3} water.
C	soil gas-phase CO_2 concentration, $\mu mol\ m^{-3}$.
c_a, c_i, c_s	CO_2 mole fraction in canopy air, at the bottom of the stomatal pore, and at the leaf surface.

c_a^{18}, $c_t^{18,sun}$, $c_t^{18,sha}$, c_g^{18} $H_2{}^{18}O$ conductances, m s^{-1}.

c_p dry air heat capacity at constant pressure, J kg^{-1} K^{-1}.

D_0 CO_2 molecular diffusitivity at 298 K, m^2 s^{-1}.

D_c, D_c^{18} CO_2 and $C^{18}OO$ effective soil diffusivity, m^2 s^{-1}.

D_w^{16}, D_w^{18} H_2O and $H_2{}^{18}O$ diffusivity, m^2 s^{-1}.

e_a, e_{atm} water vapor pressures in the plant canopy and atmosphere, Pa.

e_i, e_s leaf interior and surface water vapor pressures, Pa.

e_* saturation water vapor pressure, Pa.

E^{18} $H_2{}^{18}O$ vapor flux between the ecosystem and atmosphere, kg m^{-2} s^{-1}.

E_g^{18} soil-surface $H_2{}^{18}O$ evaporative flux, kg m^{-2} s^{-1}.

E_T transpiration flux partitioned into the soil, m^3 H_2O m^{-3} s^{-1}.

$E_v^{18,sun}$, $E_v^{18,sha}$ $H_2{}^{18}O$ fluxes from sunlit and shaded leaves, kg m^{-2} s^{-1}.

F_{al}, F_{la} CO_2 fluxes into and out of the leaf, μmol m^{-2} s^{-1}.

F_{al}^{18}, F_{la}^{18} $C^{18}OO$ fluxes into and out of the leaf, μmol m^{-2} s^{-1}.

F^{18} net ecosystem $C^{18}OO$ flux, μmol m^{-2} s^{-1}.

F_{sm}, F_g stem and growth respiration CO_2 fluxes, μmol m^{-2} s^{-1}.

F_{sm}^{18}, F_g^{18} stem and growth respiration $C^{18}OO$ fluxes, μmol m^{-2} s^{-1}.

F_{net}^{18} net $C^{18}OO$ leaf exchange, μmol m^{-2} s^{-1}.

F_s, F_s^{18} CO_2 and $C^{18}OO$ soil-surface fluxes, μmol m^{-2} s^{-1}.

f_w wetted fraction of the canopy.

I isoflux, μmol m^{-2} s^{-1} ‰.

k_H hydration rate, s^{-1}.

L leaf area index, m^2 m^{-2}.

L^{sun}, L^{sha} sunlit and shaded leaf area indices, m^2 m^{-2}.

n, n' exponents.

q soil water flux, m^3 H_2O m^{-2} s^{-1}.

q_i infiltration rate, m^3 H_2O m^{-2} s^{-1}.

p_a atmospheric pressure, Pa.

r_{aw} aerodynamic resistance between the canopy air and atmosphere, s m^{-1}.

r'_{aw} aerodynamic resistance between the soil surface and canopy air, s m^{-1}.

R_{atm}^v, R_a^v atmospheric and canopy air water vapor ^{18}O isotopic compositions.

$\bar{r}_b$ leaf boundary layer resistance, s m^{-1}.

$R_{c,atm}$ atmospheric ^{18}O isotopic ratio of CO_2.

$R_{c,l}$, $R_{c,sw}$ isotopic ratios of gaseous CO_2 in equilibrium with leaf and stem water.

R_{eq} isotopic ratio of CO_2 in equilibrium with local soil moisture.

R_g gas phase CO_2 isotopic ratio.

R_l, R_l^{sun}, R_l^{sha} leaf and sunlit and shaded leaves water isotopic ratios.

r_m soil column microbial respiration, μmol m^{-2} s^{-1}.

r_r root respiration, μmol m^{-2} s^{-1}.

R_r ^{18}O isotopic ratio of the incoming water.

R_s ^{18}O isotopic ratio of soil respired CO_2.

r_s^{sun}, r_s^{sha} sunlit and shaded stomatal resistances, s m^{-1}.

R_{sw} root density weighted soil water isotopic ratio.

R_w soil water ^{18}O isotopic ratio.

$R_{w,0}$ soil water isotopic ratio in the top soil layer.

S stem area index, m^2 m^{-2}.

S_c depth-dependent soil respiration source strength, μmol m^{-3} s^{-1}.

t time, s.

T temperature, K.

T_s soil temperature, K.

$T_{s,0}$ first soil layer temperature, K.

T_0 298 K.

T_v vegetation temperature, K.

z depth, m.

z_e e-folding distance for soil respiration, m.

α_e^c CO_2 equilibration factor.

α_e^w equilibrium vapor pressure offset.

α_k, α_{kb} $H_2{}^{18}O$ isotopic kinetic fractionations.

α_k^c, α_{kb}^c $C^{18}OO$ isotopic kinetic fractionations.

α'_k weighted kinetic fractionation across the laminar leaf boundary layer and stoma.

ε_a, ε_w air- and water-filled pore space, m^3 m^{-3} soil.

ε_t phase partitioning parameter, m^3 m^{-3} soil.

δ_{nl}^c, δ_{sw}^c, δ_s^c isotopic signatures of net leaf, stem respiration, and soil-surface CO_2 fluxes.

γ psychrometric constant, Pa K^{-1}.

κ constant for diffusion coefficient calculations.

λ latent heat of vaporization of water, J kg^{-1}.

θ soil water content, m^3 H_2O m^{-3} soil.

θ_s saturated water content, m^3 H_2O m^{-3} soil.

ρ_a air density, kg m^{-3}.
ρ_r relative rooting density.

[58] **Acknowledgments.** We thank Gordon Bonan for his publicly available and well-documented land surface model. N. McDowell and two anonymous reviewers made helpful comments on an earlier draft of the paper. This work was supported by the Atmospheric Radiation Measurement Program, Office of Science, U.S. Department of Energy under contract DE-AC03-76SF00098.

References

Alados, I., and L. Alados-Arboledas, Direct and diffuse photosynthetically active radiation: Measurements and modelling, *Agric. For. Meteorol.*, *93*, 27–38, 1999.

Amthor, J. S., *Respiration and Crop Productivity*, Springer-Verlag, New York, 1989.

Atkins, C., P. Smith, A. Mann, and P. Thumfort, Localization of carbonic anhydrase in legume nodules, *Plant Cell Environ.*, *24*, 317–326, 2001.

Baldocchi, D., A comparative study of mass and energy exchange over a closed C_3 (wheat) and an open C_4 (corn) canopy, I, The partitioning of available energy into latent and sensible heat exchange, *Agric. For. Meteorol.*, *67*, 191–220, 1994.

Bariac, T., J. Gonzalezdunia, N. Katerji, O. Bethenod, J. M. Bertolini, and A. Mariotti, Spatial variation of the isotopic composition of water (O-18, H-2) in the soil-plant-atmosphere system, 2, Assessment under field conditions, *Chem. Geol.*, *115*, 317–333, 1994.

Bird, R., W. Stewart, and E. Lightfoot, *Transport Phenomena*, 2nd ed., John Wiley, New York, 2002.

Bonan, G., A land surface model (LSM version 1.0) for ecological, hydrological, and atmospheric studies: Technical description and user's guide, *TN-417+STR*, Natl. Cent. for Atmos. Res., Boulder, Colo., 1996.

Brenninkmeier, C., K. Kraft, and W. Mook, Oxygen isotope fractionation between CO_2 and H_2O, *Isot. Geosci.*, *1*, 181–190, 1983.

Ciais, P., et al., A three-dimensional synthesis study of delta O-18 in atmospheric CO2, 1, Surface fluxes, *J. Geophys. Res.*, *102*, 5857–5872, 1997a.

Ciais, P., et al., A three-dimensional synthesis study of delta O-18 in atmospheric CO2, 2, Simulations with the TM2 transport model, *J. Geophys. Res.*, *102*, 5873–5883, 1997b.

Clapp, R., and G. Hornberger, Empirical equations for some hydraulic properties, *Water Resour. Res.*, *14*, 601–604, 1978.

Colello, G. D., C. Grivet, P. J. Sellers, and J. A. Berry, Modeling of energy, water, and CO2 flux in a temperate grassland ecosystem with SiB2: May–October 1987, *J. Atmos. Sci.*, *55*, 1141–1169, 1998.

Craig, H., and L. Gordon, Deuterium and oxygen-18 variations in the ocean and the marine atmosphere, in *Stable Isotopes in Oceanographic Studies and Paleotemperatures*, edited by E. Tongiorgi, pp. 9–130, Lischi and Figli, Pisa, Italy, 1965.

Dickinson, R. E., A. Henderson-Sellers, P. J. Kennedy, and M. F. Wilson, Biosphere/atmosphere transfer scheme (BATS) for the NCAR community climate model, *NCAR Tech. Note TN275*, Natl. Cent. for Atmos. Res., Boulder, Colo., 1986.

Farquhar, G. D., and J. Lloyd, Carbon and oxygen isotope effects in the exchange of carbon dioxide between terrestrial plants and the atmosphere, in *Stable Isotopes and Plant Carbon-Water Relations*, edited by J. R. Ehleringer et al., pp. 47–70, Academic, San Diego, Calif., 1993.

Farquhar, G. D., J. Lloyd, J. A. Taylor, L. B. Flanagan, J. P. Syvertsen, K. T. Hubick, S. C. Wong, and J. R. Ehleringer, Vegetation effects on the isotope composition of oxygen in atmospheric CO_2, *Nature*, *363*, 439–443, 1993.

Flanagan, L. B., J. P. Comstock, and J. R. Ehleringer, Comparison of modeled and observed environmental influences on the stable oxygen and hydrogen isotope composition of leaf water in Phaseolus-vulgaris L, *Plant Physiol.*, *96*, 588–596, 1991.

Flanagan, L. B., S. L. Phillips, J. R. Ehleringer, J. Lloyd, and G. D. Farquhar, Effect of changes in leaf water oxygen isotopic composition on discrimination against (Coo)-O-18-O16 during photosynthetic gas exchange, *Aust. J. Plant Physiol.*, *21*, 221–234, 1994.

Flanagan, L. B., J. R. Brooks, G. T. Varney, and J. R. Ehleringer, Discrimination against $C^{18}O^{16}O$ during photosynthesis and the oxygen isotope ratio of respired CO_2 in boreal forest ecosystems, *Global Biogeochem. Cycles*, *11*, 83–99, 1997.

Francey, R. J., and P. P. Tans, Latitudinal variation in oxygen-18 of atmospheric CO_2, *Nature*, *327*, 495–497, 1987.

Friedli, H., U. Siegenthaler, D. Rauber, and H. Oeschger, Measurements of concentration, 13C/12C and 18O/16O ratios of tropospheric carbon dioxide over Switzerland, *Tellus, Ser. B*, *39*, 80–88, 1987.

Fuller, E. N., P. D. Schettler, and J. C. Giddings, A new method for prediction of binary gas-phase diffusion coefficients, *Ind. Eng. Chem.*, *58*, 19–27, 1966.

Gillon, J. S., and D. Yakir, Naturally low carbonic anhydrase activity in C-4 and C-3 plants limits discrimination against (COO)-O-18 during photosynthesis, *Plant Cell Environ.*, *23*, 903–915, 2000a.

Gillon, J. S., and D. Yakir, Internal conductance to CO2 diffusion and (COO)-O-18 discrimination in C-3 leaves, *Plant Physiol.*, *123*, 201–213, 2000b.

Gillon, J., and D. Yakir, Influence of carbonic anhydrase activity in terrestrial vegetation on the O-18 content of atmospheric CO2, *Science*, *291*, 2584–2587, 2001.

Harwood, K. G., J. S. Gillon, A. Roberts, and H. Griffiths, Determinants of isotopic coupling of CO2 and water vapour within a Quercus petraea forest canopy, *Oecologia*, *119*, 109–119, 1999.

Helliker, B. R., and J. R. Ehleringer, Establishing a grassland signature in veins: O-18 in the leaf water of C-3 and C-4 grasses, *Proc. Natl. Acad. Sci. U.S.A.*, *97*, 7894–7898, 2000.

Hesterburg, R., and U. Siegenthaler, Production and stable isotopic composition of CO2 in soil near Bern, *Switzerland. Tellus, Ser. B*, *43*, 197–205, 1991.

Keeling, R. F., The atmospheric oxygen cycle: The oxygen isotopes of atmospheric CO2 and O-2 and the O-2/N-2 ratio, *Rev. Geophys.*, *33*, 1253–1262, 1995.

Majoube, M., Fractionnement en oxygene-18 te en deuterium entre l'eau et sa vapeur, *J. Chim. Phys.*, *58*, 1423–1436, 1971.

Mathieu, R., and T. Bariac, A numerical model for the simulation of stable isotope profiles in drying soils, *J. Geophys. Res.*, *101*, 12,685–12,696, 1996.

Merlivat, L., Molecular diffusivities of $H_2{}^{18}O$ in gases, *J. Chem Phys*, *69*, 2864–3871, 1978.

Miller, J. B., D. Yakir, J. W. C. White, and P. P. Tans, Measurement of O-18/O-16 in the soil-atmosphere CO2 flux, *Global Biogeochem. Cycles*, *13*, 761–774, 1999.

Moldrup, P., T. Olesen, T. Yamaguchi, P. Schjonning, and D.E. Rolston, Modeling diffusion and reaction in soils, IX, The Buckingham-Burdine-Campbell equation for gas diffusivity in undisturbed soil, *Soil Sci.*, *164*, 542–551, 1999.

Noone, D. C., C. J. Still, and W. J. Riley, Diagnosing impacts of changes in the biosphere by modeling 18O of atmospheric CO2 with a general circulation model, paper presented at Sixth International CO2 Conference, Cent. of Atmos. and Oceanic Stud., Grad. School of Sci., Tohoku Univ., Sendai, Japan, 2001.

Peylin, P., P. Ciais, A. S. Denning, P. P. Tans, J. A. Berry, and J. W. C. White, A 3-dimensional study of delta O-18 in atmospheric CO2: Contribution of different land ecosystems, *Tellus, Ser. B*, *51*, 642–667, 1999.

Press, W., B. Flannery, S. Teukolsky, and W. Vetterling, *Numerical Recipes (FORTRAN)*, Cambridge Univ. Press, New York, 1989.

Reindl, D. T., W. A. Beckman, and J. A. Duffie, Diffuse fraction correlations, *Sol. Energy*, *45*, 1–8, 1990.

Roden, J. S., and J. R. Ehleringer, Observations of hydrogen and oxygen isotopes in leaf water confirm the Craig-Gordon model under wide-ranging environmental conditions, *Plant Physiol.*, *120*, 1165–1173, 1999.

Sellers, P. J., D. A. Randall, C. J. Collatz, J. A. Berry, C. B. Field, D. A. Dazlich, C. Zhang, and G. D. Colello, A revised land surface parameterization (SiB2) for atmospheric GCMs, 1, Model formulation, *J. Clim.*, *9*, 676–705, 1996.

Skirrow, G., The dissolved gases: Carbon dioxide, in *Chemical Oceanography*, edited by J. P. Riley and G. Skirrow, pp. 1–92, Academic, San Diego, Calif., 1975.

Stern, L., W. T. Baisden, and R. Amundson, Processes controlling the oxygen isotope ratio of soil CO_2: Analytic and numerical modeling, *Geochim. Cosmochim. Acta*, *63*, 799–814, 1999.

Stern, L. A., R. Amundson, and W. T. Baisden, Influence of soils on oxygen isotope ratio of atmospheric CO_2, *Global Biogeochem. Cycles*, *15*, 753–759, 2001.

Suyker, A. E., and S. B. Verma, Year-round observations of the net ecosystem exchange of carbon dioxide in a native tallgrass prairie, *Global Change Biol.*, *7*, 279–289, 2001.

Tans, P. P., An observational strategy for assessing the role of terrestrial ecosystems in the global carbon cycle: Scaling down to regional levels, in *Scaling Physiological Processes: Leaf to Globe*, edited by J. R.

Ehleringer and C. B. Field, pp. 179–190, Academic, San Diego, Calif., 1993.

Tans, P. P., Oxygen isotopic equilibrium between carbon dioxide and water in soils, *Tellus, Ser. B*, *50*, 163–178, 199.

Warrick, A. W., *Soil Physics Companion*, CRC, Boca Raton, Fla., 2002.

Williams, T. G., L. B. Flanagan, and J. R. Coleman, Photosynthetic gas exchange and discrimination against (CO2)-C-13 and (COO)-O-18-O-16 in tobacco plants modified by an antisense construct to have low chloroplastic carbonic anhydrase, *Plant Physiol.*, *112*, 319–326, 1996.

Yakir, D., and X.-F. Wang, Fluxes of CO2 and water between terrestrial vegetation and the atmosphere estimated from isotope measurements, *Nature*, *381*, 515–518, 1996.

Yakir, D., J. A. Berry, L. Giles, and C. B. Osmond, Isotopic heterogeneity of water in transpiring leaves: Identification of the component that controls the delta-O-18 of atmospheric O-2 and CO_2, *Plant Cell.*, *17*, 73–80, 1994.

J. A. Berry, Department of Plant Biology, Carnegie Institution of Washington, 260 Panama Street, Stanford, CA 94305-1297, USA. (joeberry@catalase.stanford.edu)

W. J. Riley and M. S. Torn, Earth Sciences Division, Lawrence Berkeley National Laboratory, Building 90/1116, 1 Cyclotron Road, Berkeley, California, USA. (wjriley@lbl.gov; mstorn@lbl.gov)

C. J. Still, Department of Geography, University of California, Santa Barbara, 3611 Ellison Hall, CA 93106, USA. (still@sequoia.atmos.berkeley.edu)